First publ. in: Physical Review B 74 (2006), 054431

Cooling-field dependence of asymmetric reversal modes for ferromagnetic/antiferromagnetic multilayers

B. Beckmann and K. D. Usadel
Fachbereich Physik, Universität Duisburg-Essen, Lotharstrasse 1, 47048 Duisburg, Germany

U. Nowak
Department of Physics, University of York, Heslington, York YO10 5DD, United Kingdom

A numerical investigation of exchange coupled ferromagnetic/antiferromagnetic multilayers with a twinned crystal structure for the antiferromagnet is presented. Motivated by recent experimental findings we focus on the influence of the directions of the magnetic field during the initial cooling procedure and during the hysteresis. Upon variation of these directions the ferromagnet displays different reversal modes or even an asymmetric reversal with different kinds of reversal mechanisms for the decreasing and increasing branch of a single hysteresis loop. These findings can be explained within the context of the domain state model for exchange bias.

PACS number(s): 75.70.Cn, 75.40.Mg, 75.50.Lk, 85.70.−w

I. INTRODUCTION

Multilayers, or other compound materials where a ferromagnet (FM) is in contact with an antiferromagnet (AFM) often display a shift of the hysteresis loop along the magnetic field. This effect is called exchange bias (EB). Usually, this shift is observed after an initial cooling procedure where the entire system was cooled in an external magnetic field below its Néel temperature T_N of the AFM (for a review see Ref. 1). Such compound materials have been heavily investigated revealing many interesting and even striking properties besides EB itself, such as positive EB,[2,3] training effects,[3,4] asymmetrically shaped loops,[5–11] or a size dependence in nanostructured bilayers.[12]

Recent investigations within the framework of the domain state model of exchange bias[3,6,13] focused on systems which featured a uniaxial anisotropy of the AFM. The reason for this is the well-known strong uniaxial anisotropy for certain AFM in prominent EB systems.[1] Especially, it was shown that asymmetric reversal modes can occur in exchange bias systems where the AFM has only one single uniaxial anisotropy axis[6] and the origin of this effect was discussed in terms of the direction of the different effective fields which act on the FM on either sides of the loop.

However, in numerous experimental works it is emphasized that the AFM has a cubic anisotropy rather than a uniaxial,[9] or it shows a so-called twinned structure,[5,10,11,14,15] i.e., there is not one single easy axis for the AFM but rather a distribution of easy axes, which are in many cases aligned perpendicular to each other within the film plane. In these works mentioned above it is pointed out that the direction of the field during cooling with respect to the alignment of the easy axes of the AFM may have a significant impact on the kind of reversal mode which occurs during hysteresis.

For example, Fitzsimmons *et al.*[5] showed that one obtains a symmetric reversal behavior for the FM with coherent rotation on either side of the hysteresis loop when cooling and measuring the sample in a field pointing along the direction of one of the easy axes of the AFM. In contrast to that, if this is done along the direction of the bisector of both of the easy axes, an asymmetric reversal can be observed, with a coherent rotation for the decreasing and nucleation for the increasing branch of the loop. Furthermore, Tillmanns *et al.*[11] found that even for the same cooling procedure a variation of the sample orientation during the measurement leads to different reversal modes, both symmetric and asymmetric.

In order to investigate this behavior within the framework of the domain state model we need to relax the conditions of the AFM showing only a uniaxial anisotropy. The most simple approach to do so is to introduce a twin structure with two easy axes for the AFM. For simplicity, we assume that these easy axes are perpendicular to each other and within the film plane.

II. DOMAIN STATE MODEL FOR A TWIN STRUCTURE

Our simulations are based on the domain state model which was introduced earlier; for a detailed discussion of its properties see Ref. 3. In the following we consider one FM monolayer exchange coupled to a diluted AFM film consisting of 3 ML with dilution $p_{int}=0.5$ for the interface layer and $p_{vol}=0.6$ for the remaining two layers. We deliberately chose these values since these yielded the largest EB in previous simulations.

The geometry of the system we investigate deserves careful attention. The basic features are the same as described for the system with uniaxial anisotropy discussed in Ref. 3, i.e., the FM is described as a classical Heisenberg model with nearest neighbor exchange constant J_{FM}, whereas the AFM is modeled as a magnetically diluted Ising system with nearest neighbor exchange constant J_{AFM}. Unlike in previous simulations, though, we now introduce a checkerboardlike twin structure with two different easy axes for the AFM. As is shown in the sketch in Fig. 1, the AFM film is made up of patches with easy axes either aligned along the y or z axis. Each of these areas consists of 32×32 Ising spins, thus yielding a 128×128 AFM layer.

For the FM we also assume an easy axis which is aligned along the bisector of the easy axes of the AFM. The reason for this is to not favor any particular direction due to the

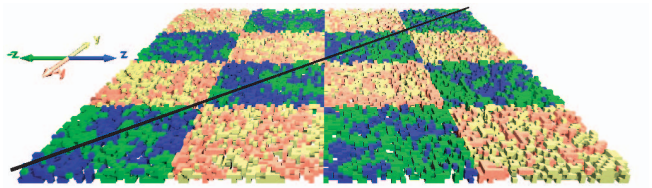

FIG. 1. (Color online) Staggered spin configuration of the AFM. The light and dark colors render the twin structure with two easy axes perpendicular to each other. One is aligned along the y axis, the other one along the z axis. The black line bisecting these two axes illustrates the direction of the easy axis of the FM.

exchange coupling to the AFM. The strength of the FM anisotropy constant is set to a value of $d=0.02J_{\mathrm{FM}}$. The dipolar interaction is approximated by an additional anisotropy term with the anisotropy constant $d_x=-0.2J_{\mathrm{INT}}$ a magnetization which is preferentially in the y-z-plane.

The Hamiltonian of our system is thus given by

$$\mathcal{H} = -J_{\mathrm{AFM}} \sum_{\langle i,j\rangle \in \mathrm{AFM}} \epsilon_i \epsilon_j \underline{\sigma}_i \underline{\sigma}_j - \sum_{i \in \mathrm{AFM}} \epsilon_i \underline{B} \underline{\sigma}_i - J_{\mathrm{FM}} \sum_{\langle i,j\rangle \in \mathrm{FM}} \underline{S}_i \cdot \underline{S}_j - \sum_{i \in \mathrm{FM}} [d(\underline{n} \cdot \underline{S})^2 + d_x S_{ix}^2 + \underline{B} \cdot \underline{S}_i] - J_{\mathrm{INT}} \sum_{\langle i \in \mathrm{AFM}, j \in \mathrm{FM}\rangle} \epsilon_i \underline{\sigma}_i \cdot \underline{S}_j, \quad (1)$$

with ϵ_i being either 1 or 0 depending on whether site i carries a magnetic moment or not. Furthermore, $\underline{S}_i$ and $\underline{\sigma}_i$ are Heisenberg and Ising spin variables at lattice side i, respectively, the first one being a classical spin vector while the latter is described as $\underline{\sigma}_i=\sigma_i \cdot \hat{\underline{y}}$ for $i \in \mathrm{AFM}_y$ or $\underline{\sigma}_i=\sigma_i \cdot \hat{\underline{z}}$ for $i \in \mathrm{AFM}_z$, where $\mathrm{AFM}_{y,z}$ denotes AFM areas with the easy axis being parallel to the y or z axis, respectively. $\underline{n}$ is the unit vector along the direction of the easy axis of the FM which is aligned along the bisector of the easy axes of the AFM as discussed before.

The first line of Eq. (1) describes the diluted AFM, the next line contains the energy contribution of the FM including nearest neighbor exchange interaction, a uniaxial anisotropy $[d(\underline{n} \cdot \underline{S})^2]$, an in-plane anisotropy $(d_x S_{ix}^2)$, and the coupling to the external field $\underline{B}$; finally the last line includes the exchange coupling across the interface between FM and AFM, where it is assumed that the Ising spins in the topmost layer of the AFM interact with the Heisenberg spins of the FM. For the nearest neighbor exchange constant J_{AFM} of the AFM which mainly determines its Néel temperature we set $J_{\mathrm{AFM}}=-J_{\mathrm{FM}}/2$. We assume the same absolute value for the coupling constant $(J_{\mathrm{INT}}=-J_{\mathrm{AFM}})$ as for the AFM.

III. MONTE CARLO SIMULATION

We use Monte Carlo methods with a heat-bath algorithm and single-spin flip methods for the simulation of the model above. The trial step of the spin update is a small variation around the initial spin for the Heisenberg model and–as usual–a single-spin flip for the Ising model.[16] We perform typically 160 000 Monte Carlo steps for a complete hysteresis loop. For the FM, we impose periodical boundary conditions within the film plane. Note that this is not necessary for the AFM since adjacent areas $\mathrm{AFM}_{y,z}$ have their easy axes perpendicular to each other, thus no interaction between these spins can occur. The external field $\underline{B}$ is within the film plane.

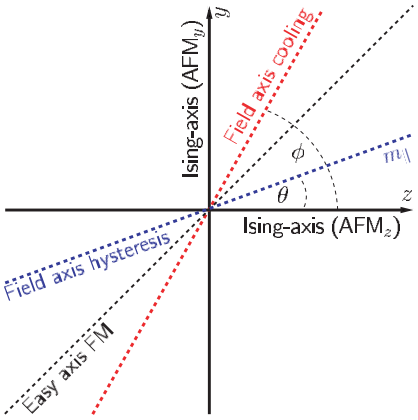

FIG. 2. (Color online) Top view of the orientation of the field axes during the initial cooling and for the hysteresis loops. The angles θ and ϕ are measured with respect to one of the easy axes of the AFM (z axis).

For the simulation of the hysteresis curves, two different angles between the external field $\underline{B}$ and the easy axis of the FM have to be distinguished (see Fig. 2). ϕ denotes the angle between $\underline{B}$ and the z axis, which is one of the easy axes of the AFM, during field cooling, whereas θ is the one which this initial angle is changed to for the simulation of the hysteresis loop itself.

In detail, the following procedure is performed to simulate the hysteresis loops for two different angles ϕ and a range of angles for θ: With the FM initially magnetized along the direction of $\underline{n}$, for cooling in an external field $|B_{\mathrm{FC}}|=0.4J_{\mathrm{FM}}$ the angle ϕ is set to either 0° or 45°, respectively. The system is cooled from its initial temperature $k_{\mathrm{B}}T=J_{\mathrm{FM}}$ to $k_{\mathrm{B}}T=0.1J_{\mathrm{FM}}$ in steps of $\Delta k_{\mathrm{B}}T=-0.002J_{\mathrm{FM}}$, which is from above to below the Néel temperature of the AFM, i.e., at each temperature step we perform 600 MCS to let the system relax. Then, hysteresis curves for different angles θ are calculated, starting with a value for the external field $B=0.32J_{\mathrm{FM}}$ which is reduced to $B=-0.32J_{\mathrm{FM}}$ in steps of $\Delta B=0.004J_{\mathrm{FM}}$ before being increased in the same manner to its initial value. Hysteresis loops for angles θ within the range of 0° to 50° in steps of 10° are calculated. We checked that for different defect realizations of the diluted AFM the same qualitative results were obtained. In the following we will focus on the reversal loops for one such defect realization.

IV. COOLING-FIELD DEPENDENCE OF REVERSAL MODES

From the results we obtained from our simulations a large variety of effects can be observed. Let us first focus on some of the most distinctive features. In particular, our simulations

show that the direction of rotation for magnetization reversal is given by the frozen AFM magnetization, depending on whether cooling took place along an AFM easy axis or along the bisector of both. Also, reversal is mostly less coherent as compared to the single crystal case and despite showing symmetric hysteresis loops both for the longitudinal and transverse components of magnetization, we sometimes observe different reversal modes when investigating the spin structure of the FM in detail. It turns out that, under certain conditions, during magnetization reversal the FM follows the local structure of the underlying AFM twin structure. Finally, for small angles ϕ the reversal behavior is close to that for the single crystal case with only one easy axis for the AFM.[6]

A. Coherent rotation vs nonuniform reversal mode

In Fig. 3 the in-plane magnetization of the FM is illustrated in the same manner as it was introduced in a recent work.[6] The magnetization reversal is plotted as m_y versus m_z, with m_z (m_y) denoting the magnetization parallel to the Ising axis of AFM_z (AFM_y). Each plot starts at the right corner corresponding to the magnetization for the maximal external field value $\underline{B}_{\max}$. Here the spins of the FM are aligned with the external field. In the left corner the magnetization points into the opposite direction when exposed to the maximal negative external field $-\underline{B}_{\max}$. Depending on whether reversal is by coherent rotation or a nonuniform reversal mode which may be characterized by a negligible transverse magnetization component, one observes either a semicirclelike shaped curve or a magnetization path more or less through the origin of the coordinate system.

Note that in our simulation thermodynamic effects are taken into account so that the magnetization magnitude depends on temperature and on its direction with respect to the easy axes and the external field. In that sense the magnetization is never fully saturated and a reversal could be called coherent when the magnetization magnitude significantly deviates from zero during reversal. Furthermore, a nonuniform reversal mode—where the magnetization magnitude breaks down to zero during reversal—might have different origins, e.g., domain wall propagation, nucleation, or even local coherent rotation. Examples for nonuniform reversal modes will be discussed later on.

In Fig. 3, a set of magnetization curves is shown for two different cooling-field directions, ϕ=0° (left) and ϕ=45° (right), and a range of angles θ. Note that since the value of the external field during cooling is much larger than the anisotropy of the FM the magnetization of the FM is always aligned with the field. One can see that for different cooling-field directions different reversal modes are obtained; most clearly this can be concluded from the magnetization curves for θ=0° shown in the first line of Fig. 3. In this case, while for ϕ=0° only a negligible transverse component is present, there is a clear coherent rotation for magnetization reversal for ϕ=45°. The reason for this behavior lies in the different frozen AFM magnetizations induced during the field-cooling process.

In the first case (left row), the cooling field is aligned parallel to one easy axis (z axis) of the AFM, thus only the

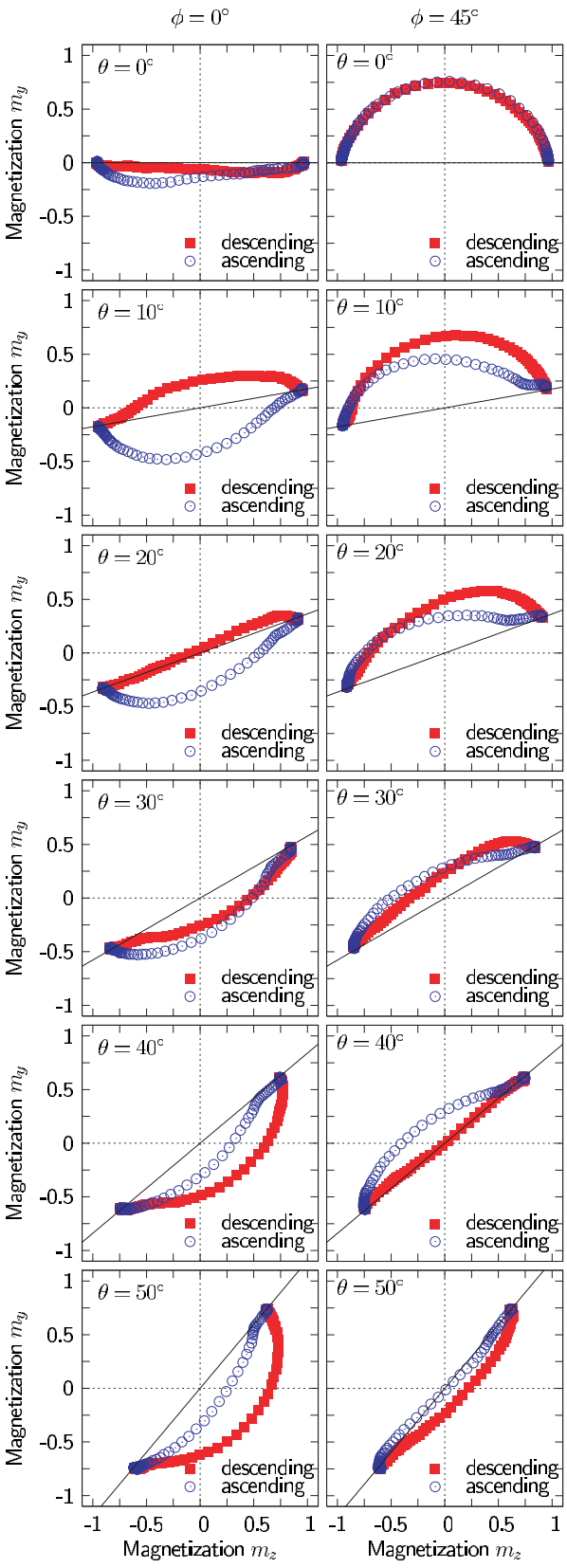

FIG. 3. (Color online) In-plane magnetization of hysteresis loops with the descending (closed squares) and ascending branch (open circles) for two different cooling-field orientations ϕ=0° (left) and ϕ=45° (right). The field axis for the hysteresis is aligned at an angle of θ for each loop as indicated.

spins with this easy axis will carry a surplus net magnetization pointing into the z direction. For the hysteresis loop with $\theta=0°$ we therefore only have a surplus net AFM magnetization parallel to the external field. Magnetization reversal for both branches of the hysteresis loop is nonuniform. Once the field for the hysteresis loop is not aligned with the z axis, there are projections of the AFM net magnetization along and perpendicular to the external field. This leads to a reversal mechanism which shows a non-negligible transverse component. For increasing angles, the AFM magnetization projection perpendicular to the applied field also increases. For $\theta=20°$ the reversal is asymmetric and finally, for $\theta \geqslant 30°$ the rotation of the magnetization is via the same side for both branches of the hysteresis loop. Qualitatively, these findings are in agreement with recent experimental results, though the range of angles where the effects above occur is different [see Fig. 2(a) of Ref. 11]. Furthermore, similar effects have been found in single-crystal systems.[6]

The second case (right row) is where the cooling field is applied along the bisector of the two easy axes. As a consequence both regions $AFM_{y,z}$ carry a net surplus magnetization. Now, even for $\theta=0°$, there already exists a non-null projection of the AFM net magnetization perpendicular to the external applied field which leads to a reversal mode predominantly characterized by a coherent rotation on either side of the hysteresis loop. Again, it is worth noting that both times the rotation is via the same direction in contrast to a pure Stoner-Wohlfarth behavior. If θ is increased now, this leads to a decreasing projection perpendicular to the external field. Therefore, the reversal mechanisms become less and less coherent before eventually there is no transverse component present any more.

B. Asymmetric magnetization reversal

From some of the magnetization curves in Fig. 3 (see, e.g., $\phi=45°$, $\theta=30°$) one cannot necessarily conclude whether the reversal mechanism for a single hysteresis loop itself shows differences for the decreasing and increasing branch of the hysteresis loop. But surprisingly, a closer look at the spin configurations of the FM for external field values close to the coercive fields reveals certain asymmetries.

In Fig. 4, as an example for a series of snapshots around the coercive fields taken from the entire hysteresis loop, two snapshots of spin configurations of the FM film during reversal for $\phi=45°$, $\theta=30°$ are shown, the top one displaying the FM close to the coercive field B^- of the decreasing branch of the hysteresis loop while the bottom one showing the same for increasing field values close to the coercive field B^+. Even though their in-plane magnetization paths in Fig. 3 do not disclose any kind of asymmetry, here it can clearly be seen that the reversal modes for decreasing and increasing fields differ significantly.

For decreasing fields the twinned structure of the underlying AFM is mapped onto the FM. Similar effects have also been found experimentally.[17,18] We obtain a reversal mode which locally shows coherent rotation depending on how the easy axis of the AFM underneath is aligned. The global magnetization of the FM film, though, has a negligible transverse

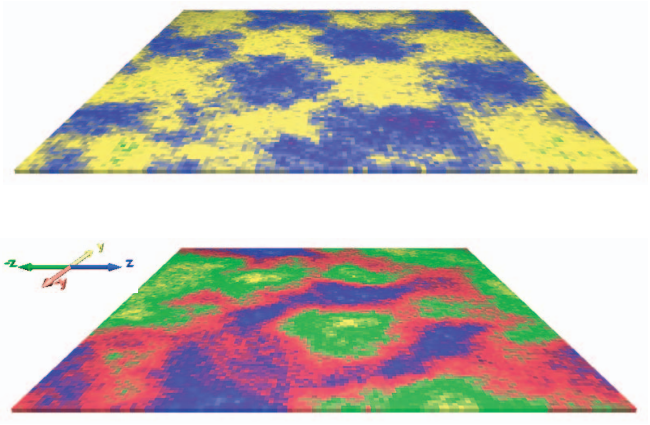

FIG. 4. (Color online) Snapshots of spin configurations of the FM monolayer close to the coercive fields B^- (top) and B^+ (bottom) for $\phi=45°$ and $\theta=30°$. In both cases a nonuniform reversal mode is observed, i.e., larger regions show coherent rotation but for different regions via opposite directions. For decreasing fields (top) the AFM twin structure is mapped onto the FM during reversal. Directions of spins are color-coded as indicated.

magnetization due to the fact that this coherent rotation is over opposite directions, thus canceling out transverse components, respectively. On the other hand, for increasing fields this behavior cannot be observed. The reversal is again nonuniform but the spin structure of the FM is not related to the underlying twinned structure of the AFM. Experimentally, asymmetric reversal modes have been found for $\theta=45°$ as well, though here the authors have observed a coherent rotation for the descending branch.[5] However, note that locally—on the length scale of the AFM twins—here we also find a coherent rotation.

The question is why such an asymmetry during the reversal can be observed with the FM showing a twinned structure during reversal only on one side of the hysteresis loop. Obviously, there is one condition that needs to be met: the domain wall width of the FM has to be considerably smaller than the average size of the AFM twins. This is indeed the case in our simulations with the provided parameters since estimating the domain wall width from $\delta=\sqrt{J/2d}$ (Ref. 19) yields a width of $\delta=5$ unit cells which is well below the size of the AFM twins with their lateral size of 32.

The reason for the asymmetry is given from the AFM interface magnetization (b) as it is shown in Fig. 5 along with the magnetization of the ferromagnetic layer (a). The regions of special interest are the ones where the external field is close to zero. Here, contributions from the external field are negligible, thus it is the AFM interface magnetization which is playing the key role.

For a decreasing external field B at remanence there is a magnetization close to $m=0.05$ for both the AFM_z and the AFM_y region. This causes the FM layer to selectively align along either direction given by the underlying AFM interface magnetization.

However, for an increasing external field B at remanence, the situation is different. The magnetization m_y in the AFM_y

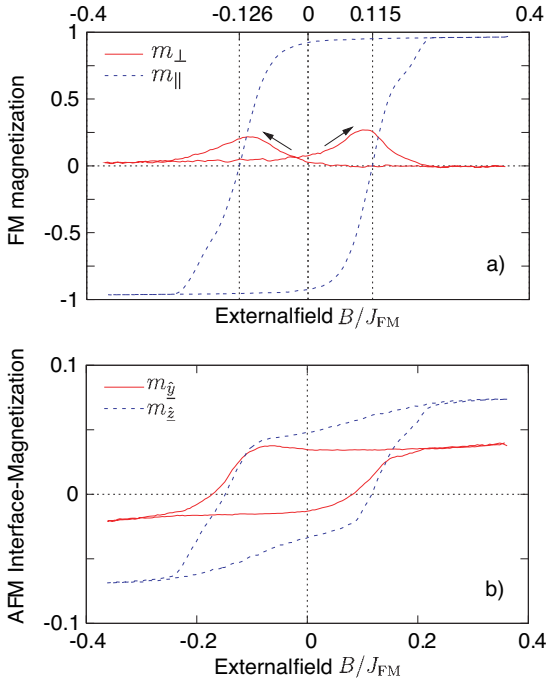

FIG. 5. (Color online) Parallel and perpendicular magnetization of the FM layer (a) and the AFM interface layer for the regions $\mathrm{AFM}_{y,z}$ (b) versus field (ϕ=45°, θ=30°).

region is close to zero, thus providing an exchange field to the FM too small to influence the FM magnetization direction significantly. Also, the regions AFM_z carry a magnetization m_z which is smaller than for decreasing fields.

V. SUMMARY

In this work we have investigated the domain state model for exchange bias. In contrast to previous simulations, rather than modeling the AFM with only one easy axis we have now introduced two easy axes in the AFM perpendicular to each other. This is the most simple approach to explore the effects of a so-called twinned structure observed experimentally. By doing so, we could show that the domain state model for exchange bias also shows a certain dependence on the direction of the external field during the field-cooling process.

This dependence could be observed when cooling along a certain direction and then measuring hysteresis loops for varying angles θ. The resulting FM in-plane magnetization curves showed distinct differences for changing directions of the cooling field.

But not only were these magnetization curves influenced by the direction of the cooling field, also the FM spin configurations during reversal revealed features which could be attributed to the twinned structure of the AFM. It showed that despite being accompanied by a rather symmetrical in-plane magnetization curve, the spin structure during reversal can be of an asymmetric kind—the twinned AFM structure mapped onto the FM on one side of the hysteresis loop, a different nonuniform reversal mode on the other.

ACKNOWLEDGMENTS

The authors would like to thank G. Güntherodt and B. Beschoten for their valuable discussions. This work was supported by the *Deutsche Forschungsgemeinschaft* through Grant No. SFB491.

[1] J. Nogués and I. K. Schuller, J. Magn. Magn. Mater. **192**, 203 (1999).
[2] C. Leighton, J. Nogués, H. Suhl, and I. K. Schuller, Phys. Rev. B **60**, 12837 (1999).
[3] U. Nowak, K. D. Usadel, J. Keller, P. Miltényi, B. Beschoten, and G. Güntherodt, Phys. Rev. B **66**, 014430 (2002).
[4] J. Keller, P. Miltényi, B. Beschoten, G. Güntherodt, U. Nowak, and K. D. Usadel, Phys. Rev. B **66**, 014431 (2002).
[5] M. R. Fitzsimmons, P. Yashar, C. Leighton, I. K. Schuller, J. Nogués, C. F. Majkrzak, and J. A. Dura, Phys. Rev. Lett. **84**, 3986 (2000).
[6] B. Beckmann, U. Nowak, and K. D. Usadel, Phys. Rev. Lett. **91**, 187201 (2003).
[7] E. Girgis, R. D. Portugal, H. Loosvelt, M. J. Van Bael, I. Gordon, M. Malfait, K. Temst, C. Van Haesendonck, L. H. A. Leunissen, and R. Jonckheere, Phys. Rev. Lett. **91**, 187202 (2003).
[8] F. Radu, M. Etzkorn, R. Siebrecht, T. Schmitte, K. Westerholt, and H. Zabel, Phys. Rev. B **67**, 134409 (2003).
[9] A. Hoffmann, Phys. Rev. Lett. **93**, 097203 (2004).
[10] M. R. Fitzsimmons, C. Leighton, A. Hoffmann, K. Liu, C. F. Majkrzak, J. A. Dura, J. R. Groves, R. W. Springer, P. N. Arendt, V. Leiner, H. Lauter, and I. K. Schuller, Phys. Rev. B **65**, 134436 (2002).
[11] A. Tillmanns, S. Oertker, B. Beschoten, G. Güntherodt, J. Eisenmenger, and I. K. Schuller, cond-mat/0509419 (unpublished).
[12] J. Eisenmenger, Z.-P. Li, W. A. A. Macedo, and I. K. Schuller, Phys. Rev. Lett. **94**, 057203 (2005).
[13] P. Miltényi, M. Gierlings, J. Keller, B. Beschoten, G. Güntherodt, U. Nowak, and K. D. Usadel, Phys. Rev. Lett. **84**, 4224 (2000).
[14] J. Nogués, T. J. Moran, D. Lederman, I. K. Schuller, and K. V. Rao, Phys. Rev. B **59**, 6984 (1999).
[15] M. J. Pechan, D. Bennett, N. Teng, C. Leighton, J. Nogués, and I. K. Schuller, Phys. Rev. B **65**, 064410 (2002).
[16] U. Nowak, in *Annual Reviews of Computational Physics IX*, edited by D. Stauffer (World Scientific, Singapore, 2001), p. 105.
[17] F. Nolting, A. Scholl, J. Stöhr, J. W. Seo, J. Fompeyrine, H. Siegwart, J.-P. Locquet, S. Anders, J. Lüning, E. E. Fullerton, M. F. Toney, M. R. Scheinfein, and H. A. Padmore, Nature (London) **405**, 767 (2000).
[18] H. Ohldag, A. Scholl, F. Nolting, S. Anders, F. U. Hillebrecht, and J. Stöhr, Phys. Rev. Lett. **86**, 2878 (2001).
[19] A. Hubert and R. Schäfer, *Magnetic Domains* (Springer-Verlag, Berlin, 1998).